Proc. Natl. Acad. Sci. USA
Vol. 77, No. 12, pp. 7209–7213, December 1980
Biochemistry

Kinetic studies of the cooperative binding of subfragment 1 to regulated actin

(tropomyosin/troponin/cooperativity)

K. M. TRYBUS AND E. W. TAYLOR

Cummings Life Science Center, University of Chicago, Chicago, Illinois 60637

Communicated by Hewson H. Swift, September 15, 1980

ABSTRACT The transient-state kinetics of binding of myosin subfragment 1 (SF-1) to regulated actin in the presence and absence of Ca^{2+} were investigated. The binding of SF-1 to pure actin, to actin–tropomyosin (actin–TM), or to actin–tropomyosin–troponin (actin–TM–TN) in the presence of Ca^{2+} was kinetically the same. In each case, the light-scattering transients were biphasic, suggesting a two-step binding of SF-1 to actin. Binding of SF-1 to regulated actin in the absence of Ca^{2+} was different from binding in its presence and also varied depending on whether SF-1 or regulated actin was in excess. The kinetic results in the absence of Ca^{2+} are explained by a cooperative binding model, in which the initial binding of SF-1 molecules to open (active) actin sites increases the number of open sites. TN-I labeled with the fluorophore 4-(*N*-iodoacetoxyethyl-*N*-methyl)-7-nitrobenz-2-oxa-1,3 diazole (TN*) was used to probe the state of the actin–TM–TN complex. Binding of SF-1 or Ca^{2+} to regulated actin (in the absence of Ca^{2+}) decreased the fluorescence of actin–TM–TN* by 30%, suggesting that binding of SF-1 or Ca^{2+} induces a similar change in state. The change in fluorescence of TN* was also used to measure the rate of the transition from the active to the relaxed state in the absence of Ca^{2+}, which was 430 sec^{-1} at 4°C in 0.1 M KCl. The lag prior to association of SF-1 with regulated actin (in the absence of Ca^{2+}) was abolished when three SF-1 molecules were prebound per seven G-actin monomers. Similarly, a titration of actin–TM–TN* (in the absence of Ca^{2+}) with SF-1 or SF-1–ADP showed that most actin sites are open, as measured by the fluorescence change, when the occupancy of actin–TM–TN* by SF-1–ADP or SF-1 is approximately 50%. The evidence shows that partial occupancy of a block of G-actin sites (possibly seven) by SF-1 or SF-1–ADP stabilizes the open (active) conformation.

Interaction of actin and myosin in skeletal muscle is regulated by the proteins tropomyosin (TM) and troponin (TN), which are located on the actin filament. Structural evidence suggests that the TM–TN complex occupies a position out of the groove of the actin helix in the absence of Ca^{2+} and may be able to sterically block the binding of myosin subfragment 1 (SF-1) to the regulated actin (1). Alternatively, the regulatory proteins may be located on the side of the actin opposite the SF-1 binding site, and the movement of TM–TN out of the groove indirectly alters the binding site for SF-1 (2). When Ca^{2+} is present, it binds to TN-C and the interaction of TN-I with actin is altered so that TM–TN occupies a position nearer the groove of the actin helix. The SF-1 binding site should be available with TM–TN in this position, and interactions between actin and myosin can occur such that the actin-activated ATPase rate is high.

The steady-state ATPase activity of regulated actin–SF-1 (3) suggests that the regulated actin filament acts as a cooperative unit. In the absence of Ca^{2+}, the ATPase activity can be activated at low ATP concentration if a fraction of the SF-1 present is not saturated with nucleotide. These so-called rigor complexes are assumed to bind to the regulated actin and displace TM–TN from its blocking position.

The kinetics of binding of SF-1 and SF-1–nucleotide complexes to regulated actin have not been investigated in detail. Recombination of a myosin–products intermediate state with regulated actin was reported to be essentially blocked in the absence of Ca^{2+} (4). In this study, we investigated the binding of SF-1 and the SF-1–ADP complex to regulated actin in the presence and absence of Ca^{2+} under a range of conditions. The observations demonstrate that the binding of SF-1 induces a cooperative activation of regulated actin. The findings are discussed in terms of a generalized steric blocking model.

MATERIALS AND METHODS

Protein Preparation. Myosin was prepared from rabbit back and leg muscles by the method of Perry (5). Actin was prepared from the acetone-dried powder as described (6). Native tropomyosin and tropomyosin were prepared according to Hitchcock (7). SF-1 was prepared from myosin by chymotryptic digestion in the presence of 1 mM EDTA as described (8). For some experiments, SF-1 was purified on DEAE-Sephacel columns and the SF-1 A-1 isoenzyme was used in the experiments. Protein concentrations were determined by UV absorbance with the following molecular weights and extinction coefficients (absorptivities): SF-1, M_r 100,000, E_{280} = 0.75 cm^2/mg; actin, M_r 42,500, E_{290} = 0.63 cm^2/mg; tropomyosin, M_r 70,000, E_{278} = 0.290 cm^2/mg; and TM–TN, M_r 148,000, E_{278} = 0.38 cm^2/mg. In each case, these absorptivities were corrected for light scattering, which was determined at 320 nm.

Fluorescent Labeling of TN. TM–TN (40 μM) was labeled by incubation with a 3-fold molar excess of 4-(*N*-iodoacetoxyethyl-*N*-methyl)-7-nitrobenz-2-oxa-1,3-diazole (IANBD) (TM–TN*) for 6 hr at 4°C and pH 7 in 30 mM KCl in the dark. IANBD was obtained from Molecular Probes (Plano, TX) and used without further purification. The reaction was terminated by addition of a 10-fold excess of 2-mercaptoethanol over label, and the sample was dialyzed overnight. The distribution of the fluorophore was determined. Duplicate 7.5% (wt/vol) Na-DodSO_4/polyacrylamide gels of TM–TN were run in the presence and absence of 2-mercaptoethanol. One gel was sliced into 19 fractions, the protein was eluted, and the fluorescence of each fraction was determined. The duplicate gel was stained with Coomassie blue and scanned in a gel scanner. The fluorescence profile was superimposed on the protein bands; 95% of the fluorescence was centered on TN-I in the presence and absence of 2-mercaptoethanol. The degree of labeling was 0.89 mol of IANBD per mol of protein, as determined from the

The publication costs of this article were defrayed in part by page charge payment. This article must therefore be hereby marked "*advertisement*" in accordance with 18 U. S. C. §1734 solely to indicate this fact.

Abbreviations: SF-1, myosin subfragment 1; TM, tropomyosin; TN, troponin; EGTA, ethylene glycol bis(β-aminoethyl ether)-*N,N,N',N'*-tetraacetic acid; IANBD, 4-(*N*-iodoacetoxyethyl-*N*-methyl)-7-nitrobenz-2-oxa-1,3-diazole; TN*, TN labeled with IANBD; Mes, 4-morpholineethanesulfonic acid.

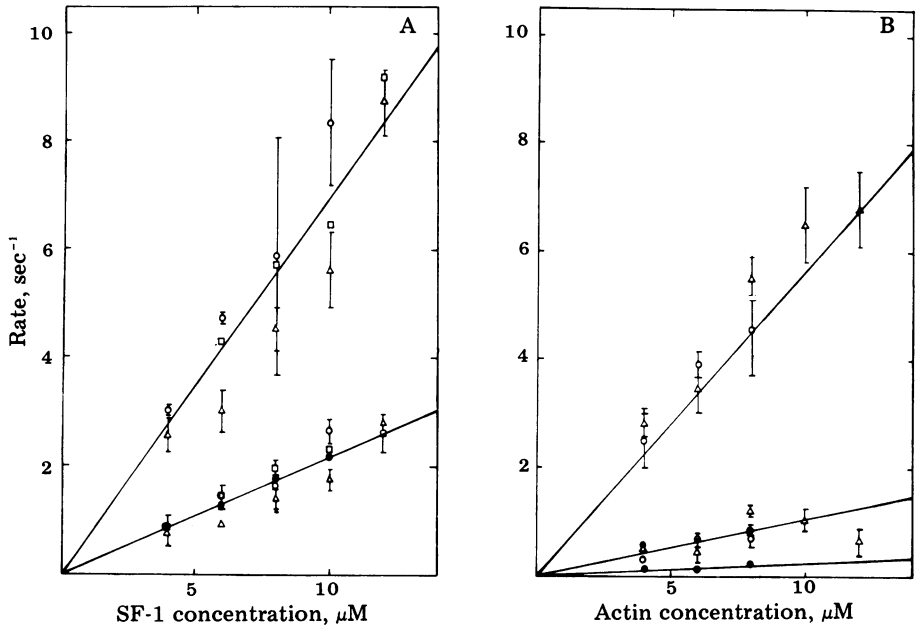

FIG. 1. Rate of binding of SF-1 to regulated actin. The rate of binding of SF-1 to pure actin (□), actin–TM (△), actin–TM–TN in the presence of Ca^{2+} (○), or actin–TM–TN in the absence of Ca^{2+} (●) after being mixed in the stopped-flow instrument is plotted as a function of SF-1 (*A*) or actin (*B*) concentration. The rates were obtained from the best fit to a single or double exponential of the light-scattering transients at 294 nm. For regulated actin in the absence of Ca^{2+} and with SF-1 in excess, the plotted rates refer to the rate of the single exponential process after the initial lag. Error bars refer to the SD of three or four experimental traces. Experimental conditions: 4°C; 10 mM Tris 4-morpholineethanesulfonic acid (Mes) (pH 7), 0.1 M KCl, 5 mM $MgCl_2$, and 100 μM $CaCl_2$ or 2 mM ethylene glycol bis(β-aminoethyl ether)-*N,N,N′,N′*-tetraacetic acid (EGTA). Final protein concentrations: 1 μM SF-1 or 1 μM actin.

absorbance at 480 nm with an extinction coefficient of 25,000 M^{-1} cm^{-1}.

Kinetic Results. Transient-state measurements were made with a stopped-flow instrument (8), and equilibrium fluorescence measurements were made with a Perkin–Elmer MPF-4 fluorescence spectrophotometer. In the stopped-flow instrument, light scattering and fluorescence of labeled actin–TM–TN* were observed simultaneously. The incident beam was passed through a 436-nm interference filter. Light scattering and fluorescence were observed at 90° to the incident beam with a 436-nm interference filter and a 550-nm cut filter, respectively. Light scattering of unlabeled actin–TM–TN was observed with an incident beam of 294 nm and recorded at 90° to the incident beam with a 290-nm interference filter. Kinetic data were fitted to either a single or a double exponential by a method of moments program adapted from the procedure of Dyson and Isenberg (9) by K. Johnson.

RESULTS

SF-1 Binding to Regulated Actin. We first investigated the rate of binding of SF-1 to pure actin, to actin–TM, and to actin–TM–TN in the presence of Ca^{2+}. The kinetic behavior was similar for the three actin species. The time course of the reaction, as measured by light scattering, fitted two exponential terms. Both rate processes increased linearly with SF-1 concentration (Fig. 1*A*). At 4°C and 0.1 M KCl, the faster process had an apparent second-order rate constant of 6–7 × 10^5 M^{-1} sec^{-1} and the slower transition was approximately one-third to one-fourth as fast. Within experimental error the rate processes were not distinguishable for the three actin species. The rate of the transient was similar whether SF-1 was in excess (Fig. 1*A*) or actin was in excess (Fig. 1*B*). The relative amplitude of the two transitions varied with protein concentration. At low SF-1 or actin concentration the transient was adequately fitted by a single exponential term. As the SF-1 or actin concentration was increased, the transients became increasingly biphasic and required a fit to two exponential terms, as shown by the two rate constants plotted in Fig. 1. The amplitude of the faster transition increased linearly with concentration and dominated the signal at high concentrations. At 5–10 μM protein, the amplitude of the faster transition was approximately three-fourths of the total signal. At very low ionic strength (30 mM KCl) the rate of the slower process approached a maximum of approximately 20 sec^{-1}.

The binding of SF-1 to regulated actin in the absence of Ca^{2+} was markedly different. With SF-1 in excess, the process showed a distinct lag; i.e., the rate of binding increased during the early part of the reaction (Fig. 2*B*). After the lag, the remainder of the association fitted a single exponential process (Fig. 1*A*, ●) of approximately the same rate as the slower

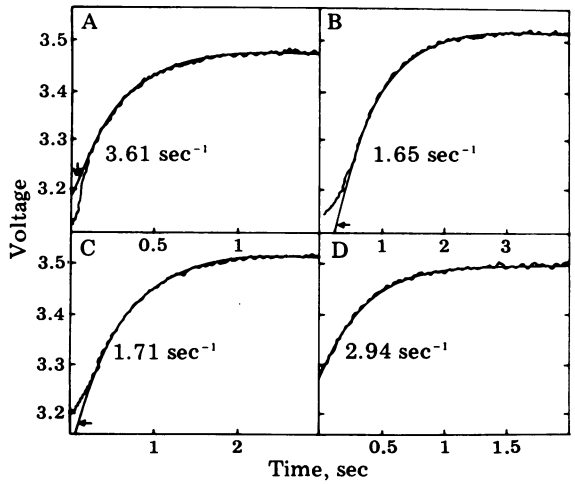

FIG. 2. Kinetics of the light-scattering transient for preloaded regulated actin in the absence of Ca^{2+}. The jagged line shows the increase in light scattering as a function of time after the mixing of actin–TM–TN* (1 μM final concentration) with a 4-fold excess of SF-1 in the stopped-flow instrument. The light-scattering transients begin at a level that is equal to the sum of the light scattering of actin and SF-1 alone. The smooth line is the computer-generated fit to a single exponential, as indicated by the arrow. (*A*) Association of SF-1 with regulated actin in the presence of Ca^{2+}; (*B*) association in the absence of Ca^{2+}. Data in *A* are fitted to a single exponential. The difference in initial slopes in the presence and absence of Ca^{2+} is approximately a factor of 10. Actin–TM–TN* was mixed with two SF-1 molecules (*C*) and four SF-1 molecules (*D*) per seven G-actin monomers before being mixed with an excess of SF-1. The lag prior to association of SF-1 with actin–TM–TN was abolished when three SF-1 molecules per seven G-actin monomers were first mixed with the regulated actin. Experimental conditions: 20°C; 10 mM Tris Mes (pH 7), 0.2 M KCl, 5 mM $MgCl_2$, and 2 mM EGTA or 100 μM $CaCl_2$.

process in the presence of Ca^{2+}. With regulated actin in excess (no Ca^{2+}), the light-scattering transient was again biphasic with no lag prior to association. However, the rates of the biphasic transient were reduced by a factor of 5–6 from the rates obtained in the presence of Ca^{2+} (Fig. 1*B*). In the absence of Ca^{2+} the main rate process had the same rate as the slower step in the presence of Ca^{2+}.

Similar results were obtained under different conditions of ionic strength and temperature. In general, the difference in the initial slope of the transient in the presence and absence of Ca^{2+} tended to increase as the ionic strength was increased, and the size of the lag phase became more pronounced.

Fluorescence Changes of Labeled Actin-TM-TN*. Troponin in which the TN-I moiety was labeled with IANBD was prepared. A regulated complex was reconstituted by using actin and TM-TN* in a 7:1 mole ratio. The addition of Ca^{2+} or SF-1 produced a 30% decrease in fluorescence emission (Table 1). Dissociation of actin-TM-TN*·SF-1 with ATP or removal of Ca^{2+} from actin-TM-TN* with EGTA restored the original level of fluorescence. Labeling of TN-I did not interfere with Ca^{2+} regulation of actin-SF-1 ATPase activity. Titration of the fluorescence signal of actin-TM-TN* by Ca^{2+} and activation of actin-TM-TM*·SF-1 ATPase by Ca^{2+} gave an apparent Ca^{2+} binding constant of $2–3 \times 10^6\ M^{-1}$ (20°C; 30 mM KCl, pH 7/5 mM $MgCl_2$). Although labeling may have altered the Ca^{2+} binding, the transition in the fluorescence signal and in the actin-activated ATPase occurred at the same Ca^{2+} concentration. The Ca^{2+} effect on the complete system is the primary concern here, but association of TM-TN* with actin in the absence of Ca^{2+} gave a 50% increase in fluorescence emission. In the presence of Ca^{2+}, the increase was 20%. Thus, interaction of TM-TN* with actin also altered the conformation of TN-I.

Because the change in fluorescence induced by Ca^{2+} and SF-1 binding has the same amplitude and both reactions correspond to activation of ATPase activity, the fluorescence emission appears to be a measure of the state of the system: the relaxed state (low ATPase, high fluorescence) in contrast to the active state (high ATPase, low fluorescence).

Rate of Transition of Regulated Actin from the Active to the Relaxed State. The fluorescence emission provides a signal for determination of the rate of the spontaneous transition from the active state to the relaxed state in the absence of Ca^{2+}. Actin-TM-TN*·SF-1, in the absence of Ca^{2+}, was mixed with various concentrations of MgATP. The TM-TN* initially is in the active, low fluorescence state, because SF-1 is bound to the regulated actin. As the MgATP dissociates the SF-1 from the regulated actin, TM-TN* returns to the relaxed, higher fluorescence state because there is no Ca^{2+} present. The rate of dissociation of the regulated actin-SF-1 by ATP and the rate of the fluorescence increase are shown in Fig. 3. The graph shows that the maximal rate of the actin transition from the active to the relaxed state is 250 sec^{-1} at 4°C and 30 mM KCl. The rate increased to 430 sec^{-1} in 0.1 M KCl but did not change measurably as the temperature was increased from 4°C to 20°C. The transition to the active state is sufficiently fast that a maximal rate of association with SF-1 was not observed in the absence of Ca^{2+}. Because the reverse transition has been shown to be very fast, it is concluded that the transition between relaxed and active actin is in rapid equilibrium during the association with SF-1.

Table 1. Amplitude of fluorescence changes of actin-TM-TN*

Reaction	Fluorescence change, %
Actin-TM-TN* (−Ca^{2+}) $\xrightarrow{+Ca^{2+}}$ Actin-TM-TN* (+Ca^{2+})	−31
Actin-TM-TN* (−Ca^{2+}) $\xrightarrow{+SF\text{-}1}$ Actin-TM-TN* · SF-1 (−Ca^{2+})	−29
Actin-TM-TN* · SF-1 (−Ca^{2+}) $\xrightarrow{+ATP}$ Actin-TM-TN* (−Ca^{2+}) + SF-1	+29
Actin-TM-TN* (+Ca^{2+}) $\xrightarrow{+EGTA}$ Actin-TM-TN* (−Ca^{2+})	+32

The changes in fluorescence after the addition of Ca^{2+}, SF-1, ATP, or EGTA to actin-TM-TN* were measured at an exciting wavelength of 436 nm (8-nm slit width) and emission wavelength of 535 nm. Only small amounts of stock solutions were added (20 μl added to 2 ml) so that the dilution effect was negligible. Experimental conditions: 20°C; 10 mM Tris Mes (pH 7), 0.1 M KCl, 5 mM $MgCl_2$, and 100 μM $CaCl_2$ or 2 mM EGTA.

Effect of Occupancy of Actin Sites on Transition from the Relaxed to the Active State. The binding of SF-1 or the binding of Ca^{2+} to regulated actin in the absence of Ca^{2+} tend to activate the regulated actin. We investigated (by two methods) the fraction of the regulated actin that must be occupied by SF-1 or SF-1–ADP to induce the transition from the relaxed to the active state. The first approach made use of the lag prior to association of SF-1 with regulated actin in the absence of Ca^{2+}. The lag is generated because, initially, only a small fraction of the actin sites can bind SF-1 (active or "open" sites), but occupancy of these sites shifts the balance in favor of open sites. The regulated actin (in the absence of Ca^{2+}) was mixed with various fractional amounts of SF-1 per seven G-actin monomers. The preloaded actin was then mixed in the stopped-flow apparatus with an excess of SF-1, and the lag prior to association was measured. A series of experimental light-scattering transients with different degrees of preloading are shown in Fig. 2. The lag prior to association was abolished when three SF-1 molecules were premixed per seven G-actin monomers. The results indicate that the binding of somewhat less than one SF-1 molecule per two G-actin monomers has shifted the equilibrium in favor of open sites.

The second approach to this problem involves the use of TM-TN*. Because the fluorescence of the labeled actin-TM-TN* complex is a measurement of the amount of open actin sites, a simultaneous titration of the fluorescence and light-scattering signals should measure the amount of open sites

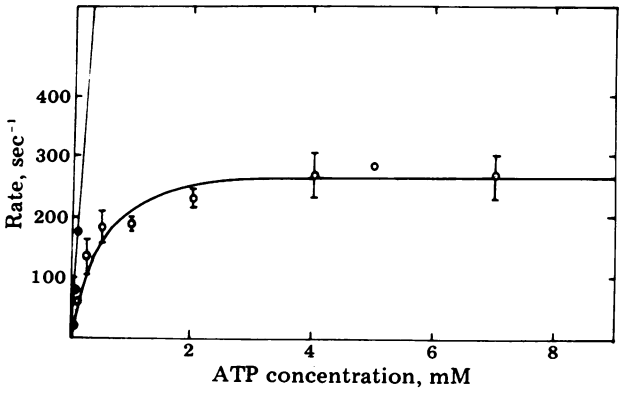

FIG. 3. Rate of the transition of regulated actin from the active to the relaxed state. The rate of dissociation by ATP (●) and the rate of the fluorescence increase (○) after mixing of 5 μM (final concentration) actin-TM-TN*·SF-1 (no Ca^{2+}) with ATP (no Ca^{2+}) in the stopped-flow instrument is plotted as a function of MgATP concentration. The rates were obtained as the best fit of the light-scattering and fluorescence transients to a single exponential. Error bars refer to the SD of three or four experimental transients. Experimental conditions: 4°C; 10 mM Tris Mes (pH 7), 30 mM KCl, 5 mM $MgCl_2$, and 2 mM EGTA.

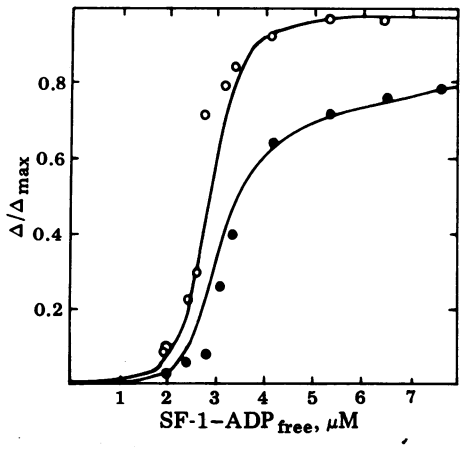

FIG. 4. Titration of the fluorescence and light-scattering changes of actin–TM–TN* with SF-1–ADP. The amplitudes of the fluorescence signal (○) and the light-scattering signal (●) were observed simultaneously in the stopped-flow apparatus after various concentrations of SF-1–ADP were mixed with actin–TM–TN* (1.3 μM final concentration). The fluorescence signal measures the fraction of open actin sites. The curves drawn through the points are calculated from a theoretical model described in the text, with a strong binding constant of 5×10^5 M^{-1}, a weak binding constant of 0, an interaction parameter Y of 5, and a block size of 7. $L'(0) = 610$, as calculated from the light-scattering curve. In the notation of ref. 10, the fluorescence signal measures p_2 and the light scattering measures θ. Experimental conditions: 20°C; 10 mM Tris Mes (pH 7), 0.2 M KCl, 5 mM $MgCl_2$, and 2 mM EGTA.

at any degree of occupancy. We first titrated actin–TM–TN* with SF-1 at 20°C and 0.1 M KCl. The fractional change of the fluorescence signal was larger than the fractional change of the light-scattering signal for all added SF-1 concentrations. A plot of the fractional change against free SF-1 concentration showed that the fluorescence change was at least 80% complete for 50% occupancy as measured by light scattering. However, the very large binding constant of SF-1 to actin leads to large errors in calculation of the free SF-1 concentration, and more accurate measurements can be made by using SF-1–ADP. Kinetic studies show an even more pronounced lag for SF-1–ADP than for SF-1. A titration curve for actin–TM–TN* with SF-1–ADP at 20°C and 0.2 M KCl is shown in Fig. 4. Under these conditions, the binding of SF-1–ADP is highly cooperative. The light-scattering signal and the fluorescence change are plotted as a function of the concentration of free SF-1–ADP. The experimental points show that when 50% of the regulated actin is occupied by SF-1–ADP, 85–90% of the sites are in the open, active configuration, as measured by the fluorescence change. The curves were calculated from a theoretical model of Hill *et al.* (10) in which nearest-neighbor interactions between tropomyosin molecules are included.

DISCUSSION

The evidence from kinetic and equilibrium experiments establishes that the binding of SF-1 and SF-1–ADP to regulated actin filaments produces a cooperative transition of the filament. It is preferable to consider the general features qualitatively before asking whether the system satisfies the requirement of the structural model of Huxley (1) or other cooperative models. Comparisons of reaction rates in the presence and absence of Ca^{2+} are complicated by the two-step binding process observed for pure actin, actin–TM, and regulated actin plus Ca^{2+}. This problem will be treated in more detail elsewhere, but the results do not appear to be a light-scattering artifact because biphasic signals are obtained with fluorescent probes on actin or SF-1. Two steps in the binding process were able to be distinguished because of improvements in signal-to-noise ratio and in computer-fitting programs. A sequential process accounts for the observations:

$$\text{Actin} + \text{SF-1} \underset{k_{-1}}{\overset{k_1}{\rightleftharpoons}} (\text{actin–SF-1})_1 \xrightarrow{k_2} (\text{actin–SF-1})_2.$$

For low concentrations of SF-1 the transient fits a single exponential term, as required by the scheme. At higher concentrations a second, slower process of small amplitude is observed (≈25% of total), and at low ionic strength (30 mM KCl or less) the slow step appears to reach a maximal rate of approximately 20 sec^{-1}. At 4°C and 30 mM KCl the transients are fitted quantitatively for the choice of constants: $k_1 = 1.5 \times 10^6$ M^{-1} sec^{-1}; $k_{-1} = k_2 = 20$ sec^{-1}. The significant point for the current studies is that an initial binding step (k_1) yields a relatively strongly bound complex and the rate of this step is approximately the same for actin, actin–TM, and regulated actin plus Ca^{2+}. This suggests that regulated actin is essentially in the strong binding state typical of pure actin.

The kinetic evidence is consistent with a two-state model, a strong binding (or open) state and a weak binding (or blocked) state. One simplifying assumption is necessary. Because the kinetic data show that the rate constant for binding to an open site is the same for pure actin and regulated actin plus Ca^{2+}, it is assumed that the rate constant for binding to an open state does not depend on the distribution of open and closed states or how that distribution is obtained (by Ca^{2+} binding, partial occupancy of the filament by SF-1, or an equilibrium between open and closed sites in the absence of Ca^{2+}).

The lower rate of binding to regulated actin in the absence of Ca^{2+} is explained by the lower concentration of strong binding sites. The ratio of the initial rates of binding in the presence or absence of Ca^{2+} with actin in large excess over SF-1 should be a measure of the fraction of strong binding sites (Fig. 1*B*). This ratio is 6; consequently, there is approximately one open site per seven G-actin residues.

The binding curves in the absence of Ca^{2+} with SF-1 in excess show an increase in rate during the early part of the reaction. Because the rate is proportional to the concentration of available actin sites, there must be a net increase in sites; therefore, SF-1 induces a cooperative transition from the relaxed to the active state of the filament. The ratio of the initial slopes of the association curves in the absence and presence of Ca^{2+} provides a second measure of the fraction of open sites, which is one out of six to eight sites.

Preloading with SF-1 eliminates the lag for an occupancy of approximately 0.4–0.5, which again indicates a cooperative transition but is not a quantitative measure of the fraction of open sites. A more detailed model is necessary to interpret the lag and the dependence of the rate constants on SF-1 concentration in Fig. 2. The results are explained quantitatively by a model in which a group of N sites is in equilibrium for the transition between relaxed ($actin_r$) and active ($actin_a$) states, and the binding constant of SF-1 to the relaxed state is sufficiently small that the binding is negligible. The equilibrium assumption is supported by the fast transition observed for fluorescent-labeled troponin and the linear dependence of the rate of binding on SF-1 concentration:

$$\text{Actin}_r \overset{K_r}{\rightleftharpoons} \text{actin}_a, \quad \text{actin}_a + \text{SF-1} \overset{Nk_1}{\rightleftharpoons} \text{actin}_a\text{–SF-1}.$$

Initially SF-1 binds to the small amount of $actin_a$ that is present. The remaining $N - 1$ sites per $actin_a$ unit remain available for binding SF-1, and additional sites in blocks of N are generated from the displacement of the $actin_r \rightleftharpoons actin_a$ equilibrium. The apparent rate constant expressed per actin residue is $K_r k_1/(K_r + 1)$, which is approximately $K_r k_1$ because K_r is small. To fit the lag and rate of association requires a value of 0.2 for K_r if

N is set equal to 7. Extension of the model to include two-step binding of SF-1 does not affect the value of K_r. The model again leads to an estimate of about one open site per six G-actins, in agreement with previous estimates. The answer is not dependent on N because the parameter that is fitted to the data is NK_r.

The simple kinetic model may not be adequate for interpreting the preloading experiment (Fig. 2). Qualitatively, the rate constant should increase and approach the value in the presence of Ca^{2+}. When four SF-1 molecules were preloaded per seven G-actin residues, the observed initial slope was 81% of that obtained in the presence of Ca^{2+}, in approximate agreement with the fraction of open sites determined from Fig. 4.

The introduction of a fluorescent label into TN-I permitted a more direct measurement of the tropomyosin–troponin transition. It is assumed provisionally that, although the fluorescence signal reports the state of troponin, there is a one-to-one correspondence with the state of tropomyosin. The assumption is plausible because the binding of Ca^{2+} to troponin and the binding of SF-1 to regulated actin induces the same change in fluorescence emission. In kinetic experiments with SF-1 or SF-1–ADP, the fractional change in fluorescence preceded the light-scattering increase. The equilibrium binding isotherm showed the cooperative transition very clearly (Fig. 4). Half of the fluorescence change was obtained at an occupancy of actin sites of 0.07–0.08, as determined by light scattering. Thus, the binding of 1 SF-1–ADP complex per 14 G-actin sites induces a transition of half of the TM–TN units to the active state. If the binding is negligible to a unit in the relaxed state, then the binding of a single SF-1–ADP complex stabilizes a unit in the active state which is the result expected for a steric model.

Greene and Eisenberg (11) have recently shown that the binding isotherm of SF-1–ADP to regulated actin is strongly cooperative and that the transition cannot be fitted by a simple two-state model with seven binding sites per cooperative unit. The studies reported here have approached the same problem primarily from a kinetic standpoint, and the measurement of the binding isotherm by light scattering is only a confirmation of their results. The authors have interpreted the binding data by means of a model that includes a second cooperative effect, the interaction of nearest-neighbor tropomyosin molecules with each other (10). (We are indebted to the authors for making their manuscript available to us prior to publication.) The fit of this model to the data is shown in Fig. 4. Because we also directly measured the cooperative transition of the TM–TN units from the fluorescence signal [the quantity p_2 of the model of Hill *et al.* (10)], we have adopted a compromise in the choice of parameters to obtain a reasonable fit to both curves. It is concluded that a better fit to the isotherm is obtained from the model of Hill *et al.* (10) than a model in which the tropomyosin interaction is omitted. The results of preliminary experiments show that the lag phase in SF-1 binding is eliminated and the slope of the binding isotherm is reduced by modification of tropomyosin to prevent end-to-end interaction between molecules. Thus, there is little doubt that an interaction between tropomyosins affects the binding of SF-1.

It is less clear that the particular model of Hill *et al.* (10) is a satisfactory description of the system. The fraction of strong binding sites (p_2) in the absence of Ca^{2+} is calculated to be $\approx 10^{-3}$ from either the data of Greene and Eisenberg (11) or our own equilibrium binding experiments, whereas the fraction of sites inferred from the kinetic evidence is larger than 10^{-1}. The kinetic estimate is less dependent on a detailed model although both treatments assume only two binding states. The kinetic model could be generalized to include interaction between the groups of sites or N could be chosen to be larger than 7 because the cooperative behavior partly depends on tropomyosin interactions, but the calculated fraction of initially open sites would not be greatly altered by these modifications of the model.

A further difficulty is the slightly "S"-shaped binding isotherm for SF-1–ADP even in the presence of Ca^{2+} (11), which leads to the prediction that the system is almost completely present in the weak binding state. Although we have obtained similar equilibrium binding curves, two other pieces of evidence suggest that in the presence of Ca^{2+}, actin–TM–TN is totally activated. First, the rate of binding of SF-1 to regulated actin in the presence of Ca^{2+} is identical to that to pure actin. No lag phase was observed, as would have been expected for a cooperative transition. Second, the amplitude of the fluorescence change of actin–TM–TN* induced by Ca^{2+} is the same as that induced by SF-1, and the latter must completely transform the system to the active state because it is stoichiometrically bound to actin.

The nearest-neighbor interaction model of Hill *et al.* is the simplest description of the system consistent with the structural evidence and the known interaction between tropomyosin units, but the predictions of the model do not appear to agree with the kinetic data. An alternative class of model would consider the tropomyosin to be flexible even when bound to actin (12), rather than treating it as a rigid rod which can be in only one of two possible states. This effectively reduces the block size of 7 to smaller values. Binding sites could be available on average in the relaxed state through motion of the molecule between the positions fixed by the interaction of troponin and actin. In this case, our assumption that the state of troponin uniquely defines the state of tropomyosin would not be valid.

The work of Greene and Eisenberg (11) and the evidence presented here have established the cooperative nature of the interaction between myosin and regulated actin. Qualitatively, the kinetic evidence is consistent with the requirements of the tropomyosin shift model of Huxley (1). However, the simplest cooperative models do not account quantitatively for the properties of the system, and further experimental and theoretical studies are necessary before we would venture to apply this evidence to an explanation of the regulation of muscle contraction.

We thank Aldona Rukuiza for excellent technical assistance and Steven Rosenfeld for determining the location of the IANBD fluorophore. This work was supported by Program Project Grant HL 20592 from the National Institutes of Health and a grant from the Muscular Dystrophy Association of America.

1. Huxley, H. E. (1972) *Cold Spring Harbor Symp. Quant. Biol.* **37**, 361–376.
2. Seymour, J. & O'Brien, E. J. (1980) *Nature (London)* **283**, 680–682.
3. Bremel, R. D., Murray, J. M. & Weber, A. (1972) *Cold Spring Harbor Symp. Quant. Biol.* **37**, 267–275.
4. Koretz, J. F., Hunt, T. & Taylor, E. W. (1972) *Cold Spring Harbor Symp. Quant. Biol.* **37**, 179–184.
5. Perry, S. V. (1955) *Methods Enzymol.* **2**, 582–588.
6. Taylor, R. S. & Weeds, A. G. (1976) *Biochem. J.* **159**, 301–315.
7. Hitchcock, S. E. (1973) *Biochemistry* **12**, 2509–2515.
8. Johnson, K. A. & Taylor, E. W. (1978) *Biochemistry* **17**, 3432–3442.
9. Dyson, R. D. & Isenberg, I. (1971) *Biochemistry* **10**, 3233–3241.
10. Hill, T. L., Eisenberg, E. & Greene, L. E. (1980) *Proc. Natl. Acad. Sci. USA* **77**, 3186–3190.
11. Greene, L. E. & Eisenberg, E. (1980) *Proc. Natl. Acad. Sci. USA* **77**, 2616–2620.
12 Phillips, G. N., Jr., Lattmon, E. E., Cummins, P., Lee, K. Y. & Cohen, C. (1979) *Nature (London)* **278**, 413–417.